Journal of Magnetic Resonance **146,** 283–289 (2000)
doi:10.1006/jmre.2000.2158, available online at http://www.idealibrary.com on IDEAL®

Cross-Relaxation Effects in Stimulated-Echo-Type PGSE NMR Experiments by Bipolar and Monopolar Gradient Pulses

S. V. Dvinskikh[1] and I. Furó[2]

Division of Physical Chemistry, Department of Chemistry, Royal Institute of Technology, SE-10044 Stockholm, Sweden

Received April 19, 2000; revised June 30, 2000

Exchange of longitudinal spin polarization by dipolar cross relaxation between nonequivalent spins results in a modulation of the stimulated echo signal on increasing the encoding/decoding delays and in a multiexponential decay on increasing the diffusion time. These artifacts are suppressed by 180° pulses inserted in the middle of the gradient encoding/decoding periods. The efficiency of the gradient encoding is preserved if bipolar gradient pulses are used instead of monopolar pulses. The behavior of the different pulse sequences is demonstrated by ^{19}F PGSE NMR experiments in a lyotropic liquid crystal in both isotropic micellar and oriented nematic phases.

Key Words: **cross-relaxation; PGSE NMR; stimulated echo; bipolar gradients.**

INTRODUCTION

Many of the PGSE-type NMR methods (*1–5*), widely applied to study molecular self-diffusion, are based on the stimulated echo sequence (STE) (*6*). The advantage with STE (see Fig. 1a) is that the diffusion time Δ can be extended up to the longitudinal relaxation time T_1. This is particularly useful in many colloidal (*7*) systems where $T_1 \gg T_2$ (T_2 is the transverse relaxation time). For noninteracting spins, the magnetization during (most of) Δ is influenced solely by longitudinal relaxation that can be usually approximated as single exponential. However, *J* coupling, chemical exchange or dipolar cross relaxation may lead to a more complex behavior as in the closely related NOESY and EXSY spectroscopies (*8*) that are based on the same rf pulse sequence as STE-type PGSE (or PGSTE) NMR.

The influence of *intermolecular* transfer of longitudinal spin polarization by chemical exchange on the result of an STE experiment was investigated in detail (*9*), particularly for transfers between larger (slowly diffusing) and smaller (quickly diffusing) molecules (*10, 11*). The same formalism can be used for evaluating the effects of cross relaxation. Chemical exchange among environments with distinct chemical shifts was demonstrated to affect the STE experiment (*12*) by introducing a modulation of the signal on increasing the encoding/decoding times. Analogous modulation has been demonstrated in the case of *intramolecular* polarization transfer by cross relaxation (*13, 14*).

Below we shall further investigate such a modulation affected by intramolecular cross relaxation. More importantly, we shall draw attention to another effect: distinctly nonexponential decay of the signal on increasing the diffusion time Δ, which is in contrast to the expected behavior of STE for unrestricted diffusion (*6*). As a consequence, STE results obtained on cross-relaxing nuclei can be easily misinterpreted as restricted or anomalous diffusion even in the absence of those phenomena. Moreover, cross relaxation, chemical exchange, or spin-diffusion via static dipole–dipole coupling may severely affect those diffusion experiments that, by necessity, must vary the diffusion time Δ instead of the strength (or the length) of the encoding/decoding gradient pulses. Two examples are diffusion experiments in a static gradient (*15*) and PGSE methods incorporating dipolar decoupling (*16–18*) that are influenced even when the chemical shift differences in a spectrum are masked by a strong dipole–dipole coupling. In particular, cross relaxation (or spin diffusion via static dipole–dipole coupling) is often strong enough in colloidal systems to compromise the STE method. To avoid this, appropriate 180° pulses are inserted as indicated in Fig. 1b (*14, 19, 20*) while monopolar gradient pulses are replaced bipolar ones. Below, we present detailed calculations and experiments to illustrate the efficacy of this remedy.

THEORY

The rf pulse sequence of the STE experiment, i.e., $90_{\phi 1}$–τ_1–$90_{\phi 2}$–τ_m–$90_{\phi 3}$–τ_2 introduced in Fig. 1 and under Experimental, is the same as that for NOESY and EXSY spectroscopies (*8, 21, 22*). We limit our attention to the response of a homonuclear two-spin system within the same molecule to the STE experiment in which the field gradient *g* is applied along the *z* axis. We assume that an appropriate phase cycle (*8*) or spoiling gradient selects coherence transfer pathways that involve only

[1] On leave from the Institute of Physics, St. Petersburg State University, 198904 St. Petersburg, Russia.

[2] To whom correspondence should be addressed: Fax: +46 8 7908207. E-mail: ifuro@physchem.kth.se.

1090-7807/00 $35.00

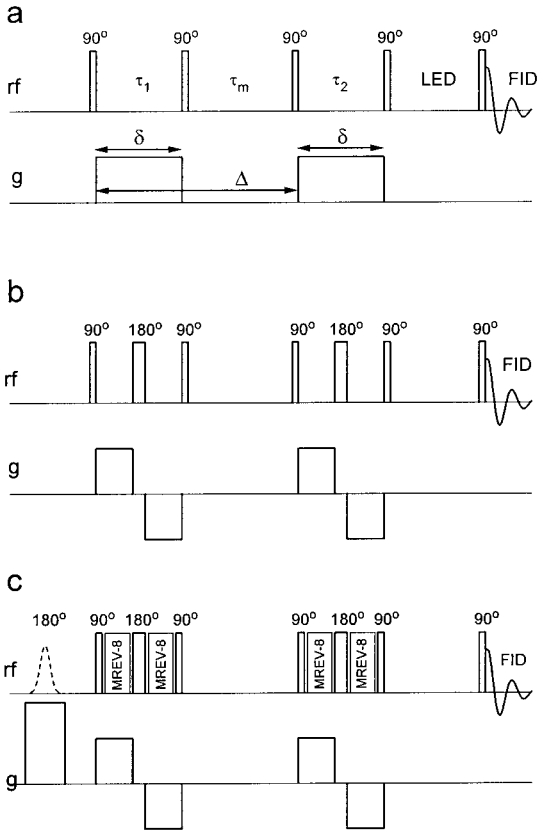

FIG. 1. PGSE NMR with a stimulated echo: (a) the conventional pulse sequence with monopolar gradient pulses and LED (*23*), (b) The pulse sequence with 180° pulses and bipolar gradient pulses inserted into the encoding/decoding periods, and (c) the pulse sequence with MREV-8 homonuclear dipolar decoupling and slice selection (*18*) and bipolar gradient pulses. A routine phase cycle (first 90° pulse $+x$, $-x$; second and third 90° pulses $2(+x)$, $2(+y)$, $2(-x)$, $2(-y)$; fourth and fifth 90° pulses $8(+x)$, $8(-x)$; receiver $+x$, $2(-x)$, $+x$) was applied in the sequence in (a). In (b) and (c), the phases of both 180° pulses were set to $+x$, and the receiver phase was changed to $+x$, $-x$. In (c), the slice selection is performed before the stimulated echo sequence with a Gaussian inversion pulse during an additional gradient pulse. The phase cycle is repeated twice with and without the inversion pulse (with phase $+x$) and the receiver phase is inverted in the subsequent cycles.

longitudinal spin polarizations during the τ_m period. As a further limitation, we treat the case without J coupling.

As compared to the well-known solution to the problem of two cross-relaxing spins we have the following complications. First, the frequency by which the single-quantum coherences belonging to the two spins evolve during the τ_1 and τ_2 periods are position dependent and expressed as

$$\omega_i(z) = \omega_i + \gamma g z, \qquad [1]$$

where ω_i denotes the two distinct chemical shifts of the spins involved. Note that the gradient pulses in Fig. 1a are assumed to fill the τ_1 and τ_2 periods; if they are set shorter Eq. [1] is still valid but with the gradient strength scaled by $\delta/\tau_{1,2}$. An important consequence of Eq. [1] is that the initial condition for dipolar cross relaxation during τ_m varies along z. Second, signal damping by diffusion is described by adding new terms to the conventional dipolar relaxation matrix (*8, 21, 22*) as

$$\mathbf{R} = -\begin{pmatrix} \rho_1 + q^2 D & \sigma \\ \sigma & \rho_2 + q^2 D \end{pmatrix}, \qquad [2]$$

where $q = \gamma g \delta$ with δ being the length of the gradient pulse and D the diffusion coefficient, and ρ and σ are the dipolar diagonal and cross-relaxation terms. This approximation is valid if $\tau_1, \tau_2 \ll \tau_m$. Under the conditions in Eqs. [1] and [2], the magnetization for the two involved spins at the end of the pulse sequence 90_x–τ_1–$90_{\pm x}$–τ_m–$90_{\pm x}$–τ_2 (see Fig. 1a) can be expressed as

$$\begin{pmatrix} M_1(\tau_1, \tau_m, \tau_2) \\ M_2(\tau_1, \tau_m, \tau_2) \end{pmatrix} = \int \left\{ \frac{1}{2} \begin{pmatrix} \pm e^{i\omega_1(z)\tau_2} & 0 \\ 0 & \pm e^{i\omega_2(z)\tau_2} \end{pmatrix} \times \begin{pmatrix} [\epsilon_- e^{\lambda_+ \tau_m} + \epsilon_+ e^{\lambda_- \tau_m}] & -\frac{\sigma}{\mu}[e^{\lambda_+ \tau_m} - e^{\lambda_- \tau_m}] \\ -\frac{\sigma}{\mu}[e^{\lambda_+ \tau_m} - e^{\lambda_- \tau_m}] & [\epsilon_+ e^{\lambda_+ \tau_m} + \epsilon_- e^{\lambda_- \tau_m}] \end{pmatrix} \times \begin{pmatrix} \pm\cos(\omega_1(z)\tau_1) & 0 \\ 0 & \pm\cos(\omega_2(z)\tau_1) \end{pmatrix} \begin{pmatrix} m_{02} \\ m_{01} \end{pmatrix} \right\} dz \qquad [3a]$$

and as

$$\begin{pmatrix} M_1(\tau_1, \tau_m, \tau_2) \\ M_2(\tau_1, \tau_m, \tau_2) \end{pmatrix} = \int \left\{ \frac{1}{2} \begin{pmatrix} \pm i e^{i\omega_1(z)\tau_2} & 0 \\ 0 & \pm i e^{i\omega_2(z)\tau_2} \end{pmatrix} \times \begin{pmatrix} [\epsilon_- e^{\lambda_+ \tau_m} + \epsilon_+ e^{\lambda_- \tau_m}] & -\frac{\sigma}{\mu}[e^{\lambda_+ \tau_m} - e^{\lambda_- \tau_m}] \\ -\frac{\sigma}{\mu}[e^{\lambda_+ \tau_m} - e^{\lambda_- \tau_m}] & [\epsilon_+ e^{\lambda_+ \tau_m} + \epsilon_- e^{\lambda_- \tau_m}] \end{pmatrix} \times \begin{pmatrix} \pm\sin(\omega_1(z)\tau_1) & 0 \\ 0 & \pm\sin(\omega_2(z)\tau_1) \end{pmatrix} \begin{pmatrix} m_{02} \\ m_{01} \end{pmatrix} \right\} dz \qquad [3b]$$

at the end of the sequence 90_x–τ_1–$90_{\pm y}$–τ_m–$90_{\pm y}$–τ_2 (*8, 21*). Note that the "longitudinal eddy delay" (LED) (*23*) part at the end of the pulse sequences in Fig. 1 only multiplies the detected signal by a constant factor. In Eq. [3], m_{0i} is the equilibrium magnetization per unit length in the z direction, $\rho_- = \rho_1 - \rho_2$, $\rho_+ = \rho_1 + \rho_2 + 2q^2 D$, $\mu = (\rho_-^2 + 4\sigma^2)^{1/2}$, $\lambda_\pm = \frac{1}{2}(-\rho_+ \pm \mu)$, $\epsilon_\pm = 1 \pm \rho_-/\mu$, and the integration is performed over the sample volume. If required, that volume can be limited by slice selection.

Setting $\tau_1 = \tau_2 \equiv \tau$, the signal intensity (the integral of the absorption signal) for 90_x–τ_1–$90_{\pm x}$–τ_m–$90_{\pm x}$–τ_2 becomes

$$S_1(\tau, \tau_m) = (\mathrm{Re}(M_1(\tau, \tau_m)) = -\frac{1}{2}[\epsilon_- e^{\lambda_+\tau_m} + \epsilon_+ e^{\lambda_-\tau_m}] \times \left[1/2 + 1/2 \int \cos((2\omega_1 + 2\gamma g z)\tau) dz\right] M_{01} + \frac{1}{2}\frac{\sigma}{\mu}[e^{\lambda_+\tau_m} - e^{\lambda_-\tau_m}]\left[1/2\ \cos((\omega_2 - \omega_1)\tau) + 1/2 \int \cos((\omega_2 + \omega_1 + 2\gamma g z)\tau) dz\right] M_{02} \quad [4a]$$

with an analogous expression for $S_2(\tau, \tau_m)$. For 90_x–τ_1–$90_{\pm y}$–τ_m–$90_{\pm y}$–τ_2 we obtain instead

$$S_1(\tau, \tau_m) = (\mathrm{Re}(M_1(\tau, \tau_m)) = -\frac{1}{2}[\epsilon_- e^{\lambda_+\tau_m} + \epsilon_+ e^{\lambda_-\tau_m}] \times \left[-1/2 + 1/2 \int \cos((2\omega_1 + 2\gamma g z)\tau) dz\right] M_{01} + \frac{1}{2}\frac{\sigma}{\mu}[e^{\lambda_+\tau_m} - e^{\lambda_-\tau_m}]\left[-1/2\ \cos((\omega_2 - \omega_1)\tau) + 1/2 \int \cos((\omega_2 + \omega_1 + 2\gamma g z)\tau) dz\right] M_{02} \quad [4b]$$

with $M_{0i} = m_{0i} \times l$ where l is the sample length. The integral terms in Eq. [4] vanish from the final result both since the phase cycle (see Fig. 1a) results in the subtraction (i.e., cancellation) of the integral terms in Eqs. [4a] and [4b] and because for $g \gg 2\pi/(\gamma l \tau)$, the individual integrals vanish. Hence, adding the contributions from the individual experiments of the four-step basic cycle we obtain

$$S_1(\tau, \tau_m) = -[\epsilon_- e^{\lambda_+\tau_m} + \epsilon_+ e^{\lambda_-\tau_m}] M_{01} + \frac{\sigma}{\mu}[e^{\lambda_+\tau_m} - e^{\lambda_-\tau_m}]\cos((\omega_2 - \omega_1)\tau)\, M_{02}. \quad [5]$$

The second term in Eq. [5] leads to a modulation of the signal on increasing the time τ for the coherence evolution (*11, 13*). Nevertheless, in an experiment performed with increasing gradient strength for a particular value of τ the decay of the signal follows the conventional Gaussian expression $S(g) \sim \exp(-\mathrm{const} \times g^2)$, albeit with a reduced signal intensity. Optimal conditions for a diffusion experiment exist at the maxima of the expression in Eq. [5] at $\tau = 2\pi/(\omega_2 - \omega_1)$ (for more than two involved spins it is more difficult to find favorable conditions). If the chemical shift range is small (e.g., for ^{1}H nuclei), τ, while sufficiently long for inserting a gradient pulse, may be set to $\tau \ll \pi/(\omega_2 - \omega_1)$ with a negligible loss of signal intensity.

From Eq. [5] it can also be seen that the signal decays in a double-exponential fashion with increasing τ_m. The exact appearance of the decay depends on the chemical shift difference $(\omega_2 - \omega_1)$ and the selected τ. The diffusion damping term dominates only at large gradients when $q^2D \gg \rho_-$ and $q^2D \gg \sigma$, in which case the decay is single exponential $\sim\exp(-q^2D\tau_m)$ (*6*) and the diffusion coefficient can be measured by varying τ_m (*15–18*).

These complications can be suppressed if a 180° pulse, applied at the middle of the first evolution period, refocuses the chemical shift evolution. To preserve the encoding by the applied gradient, the gradient polarity is simply reversed after the refocusing pulse as shown in Fig. 1b; for symmetry reasons, the same construction (*14, 19, 20*) also replaces the gradient pulse during τ_2. The signal in this experiment can be obtained by replacing $\omega_i(z)$ everywhere in Eq. [3] with $\gamma g z$, from which it follows that

$$S_1(\tau, \tau_m) = -[\epsilon_- e^{\lambda_+\tau_m} + \epsilon_+ e^{\lambda_-\tau_m}] M_{01} + \frac{\sigma}{\mu}[e^{\lambda_+\tau_m} - e^{\lambda_-\tau_m}] M_{02} \quad [6]$$

is obtained instead of Eq. [5]. Clearly, the signal is not modulated as τ increases and any τ can be chosen without loss of signal. The signal still decays in a double-exponential fashion with increasing τ_m but the deviation from a single-exponential decay is much reduced. This is a consequence of the identical initial conditions for the longitudinal magnetizations at the two sites after the second rf pulse. Hence, the transfer of longitudinal magnetization among them is only driven by the magnetization difference between the two sites that is caused by relaxation. In particular, with $\rho_1 = \rho_2 = \rho$ and $M_{01} = M_{02}$ Eq. [6] reduces to the conventional single-exponential decay $S(\tau_m) \sim \exp(-(\rho + \sigma + q^2D)\tau_m)$.

RESULTS AND DISCUSSION

The cross-relaxation effects discussed above are experimentally demonstrated by ^{19}F PGSE NMR in the lyotropic mixture of cesium perfluorooctanoate (CsPFO) with D_2O both in the isotropic micellar and anisotropic nematic phases oriented in the applied magnetic field (*24*). The spectra in those two phases are shown in Fig. 2; note that the spectrum of the nematic phase has been recorded under homonuclear decoupling (without decoupling, the spectrum is around 16 kHz wide (*18*)). Both the assignment (*25*) and the explanation of the apparent chemical shift differences between the two phases (*17*) are as previously communicated. The cross relaxation among the various ^{19}F spins along the perfluoroalkyl chain is rather fast (*25*), in particularly at low temperatures where the orientational

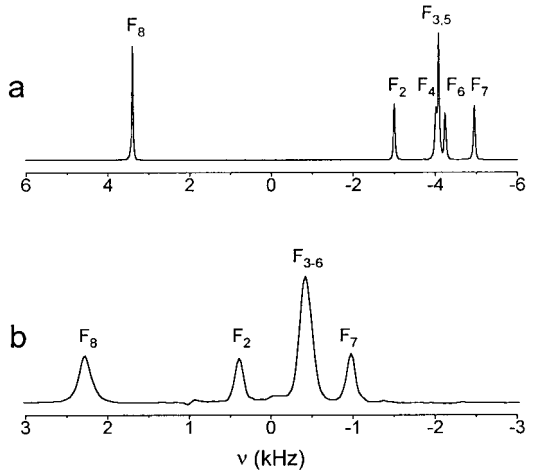

FIG. 2. ^{19}F NMR spectra of the mixture of cesium perfluorooctanoate (CsPFO) with D_2O (at 40 wt%) (a) in the isotropic micellar phase at 328 K and (b) in the nematic phase at 304 K, both recorded at 188 MHz with the same rf offset. The nematic sample is uniformly oriented by the magnetic field with its director parallel to the field direction. Spectrum (b) is recorded in the presence of MREV-8 homonuclear decoupling with 2.6-μs 90° pulse length and 84-μs cycle time; the frequency scale is not corrected by the scaling factor s ($\approx$0.5) of the decoupling sequence (*28*). The F_i signal belongs to the ^{19}F atoms attached to the ith carbon in the perfluorooctanoate chain with F_8 corresponding to the trifluoromethyl group at the end.

fluctuation of the micelles is slower. This is demonstrated in Fig. 3 with the NOESY spectra recorded at 328 K (23 K above the nematic-isotropic phase transition) and at 306 K (1 K above the phase transition) with the same mixing time (1 s). The cross peaks are positive as expected for the slow motion limit (*22*) and increase with decreasing temperature.

The actual pulse sequences are shown in Fig. 1. The conventional STE experiment, supplemented by LED (*23*), in Fig. 1a is widely used in isotropic liquids. The results of applying it to the ^{19}F spins in the isotropic micellar phase of CsPFO/D_2O are shown in Figs. 4a–4d; the present data were obtained using the F2 resonance (Fig. 2a). For simplicity, the applied gradient was set to $g = 2$ G/cm, which results in a complete coherence dephasing during the evolution time τ but is too weak to produce a significant diffusion damping. Hence, the decay of the signal is solely due to spin relaxation. At high temperature (Fig. 4a), a single-exponential decay of the signal is observed on increasing the diffusion time Δ by increasing τ_m. The decay constant of 0.96 s is close to the longitudinal relaxation time $T_1 = 1.01$ s, measured independently in an inversion-recovery experiment. On increasing τ instead, weak oscillations that can be attributed to weak cross relaxation as demonstrated in the NOESY spectrum in Fig. 3a are detected (Fig. 4b). At low temperature, however, the decay with increasing Δ is clearly nonexponential (Fig. 4c), and a strong oscillation (Fig. 4d) is observed with increasing τ. The oscillation frequency of 1.05 kHz is close to the chemical shift difference $\Delta\nu = 1.06$ kHz between the F_2 and $F_{3,4,5}$ (unresolved at 306 K) fluorine peaks. The cross relaxation among those sites is strong as can be seen in NOESY spectrum in Fig. 3b. Both of these artifacts are suppressed if one uses the pulse sequence in Fig. 1b as shown in Figs. 4e and 4f. The decay time of 0.99 s (Fig. 4e), obtained by a single-exponential fit, is close to the longitudinal relaxation time $T_1 = 1.00$ s measured in an inversion-recovery experiment.

Figure 5 demonstrates the usefulness of the inserted 180° pulses (and bipolar gradients) in an experimental situation where the diffusion coefficient is obtained from recording the decay of the signal by increasing the diffusion time Δ. The data are obtained by the PGSE sequence (Fig. 1c) with homonuclear decoupling (*18*) in the nematic phase of the CsPFO/D_2O mixture. Since the homonuclear decoupling suppresses flip–flop spin diffusion caused by the static dipole–dipole coupling among the fluorine spins, the cross-relaxation behavior (caused by that part of the dipole–dipole coupling that is rendered fluctuating by molecular motions) is expected to be similar to that in the isotropic micellar phase. To avoid heating problems, PGSE experiments with homonuclear decoupling may dispense with decoupling during the long acquisition period. In that case, one cannot record, as in Fig. 4, the decay of the signal belonging to a particular fluorine atom. Hence, Fig. 5 displays

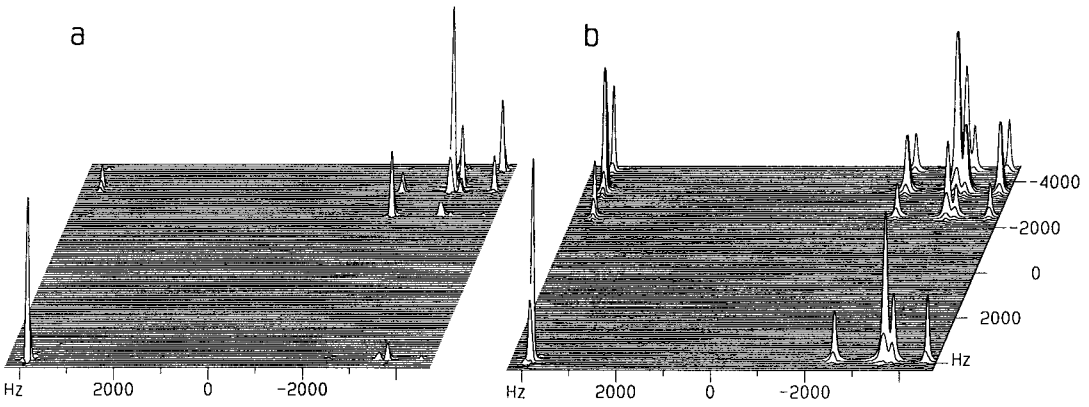

FIG. 3. Two-dimensional ^{19}F NOESY spectra of CsPFO/D_2O in the isotropic micellar phase at (a) 328 K and (b) 306 K, with the mixing time τ_m set to 1 s.

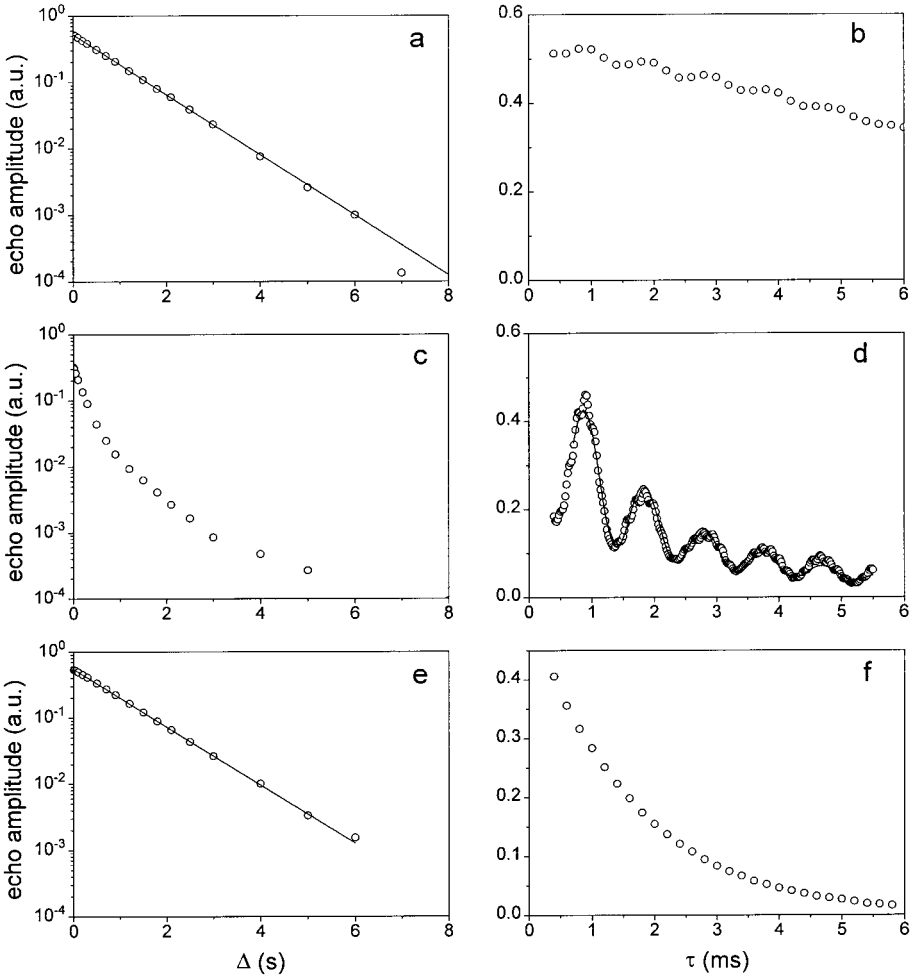

FIG. 4. Variation of the ^{19}F signal intensity of the F2 resonance (see spectrum in Fig. 2a) of CsPFO/D_2O in the isotropic micellar phase at 328 K (a, b) and at 306 K (c–f). The data are recorded with the pulse sequences in Fig. 1a (a–d) and Fig. 1b (e, f). In the first column (a, c, e) Δ is varied at constant $\tau = 1.8$ ms, while in the second column (b, d, f) τ is varied at constant $\Delta = 100$ ms. The lines are single-exponential fits, while the line in (d) is the result of regression of Eq. (5) onto the data.

the decay of the intensity of the dipolar-broadened full spectrum. Nevertheless, nonexponential (Fig. 5a) and oscillatory (Fig. 5b) decays are found as expected, although there is clearly more than one frequency present. The discernable oscillation frequencies are in the range of the frequency differences in the homodecoupled spectrum (Fig. 2b). The results obtained by bipolar gradients are presented in Figs. 5c and 5d. The obtained decay time of 0.96 s (Fig. 5c) agrees well with the longitudinal relaxation times $T_1 = 0.98$ s measured by inversion recovery.

CONCLUSION

Bipolar gradient pulses surrounding a 180° rf pulse are preferred to monopolar gradient pulses for several reasons. The original motivation for introducing this construction into the stimulated-echo-type experiments stems from the advantages brought in by the bipolar gradients: reduced eddy currents, less disturbance of the lock signal during the gradient pulses (*20*), and elimination of the effects of background gradients (*19*). In those designs, the 180° pulses were inserted to enable encoding/decoding by bipolar gradients. It has been indicated only recently that those 180° pulses may also suppress disadvantageous cross-relaxation effects in stimulated-echo-type PGSE experiments (*14*). Of those effects, oscillations on increasing the encoding/decoding time τ may lead to a severe loss of signal that decreases the precision of the obtained diffusion coefficients. A more serious problem is the nonexponential variation of the signal on increasing the diffusion time Δ. This effect may cause systematic errors in the diffusion coefficients obtained by variable-diffusion-time methods. Moreover, the observed nonexponentiality may be readily misinterpreted as a sign of restricted or anomalous diffusion. Both of these sets of

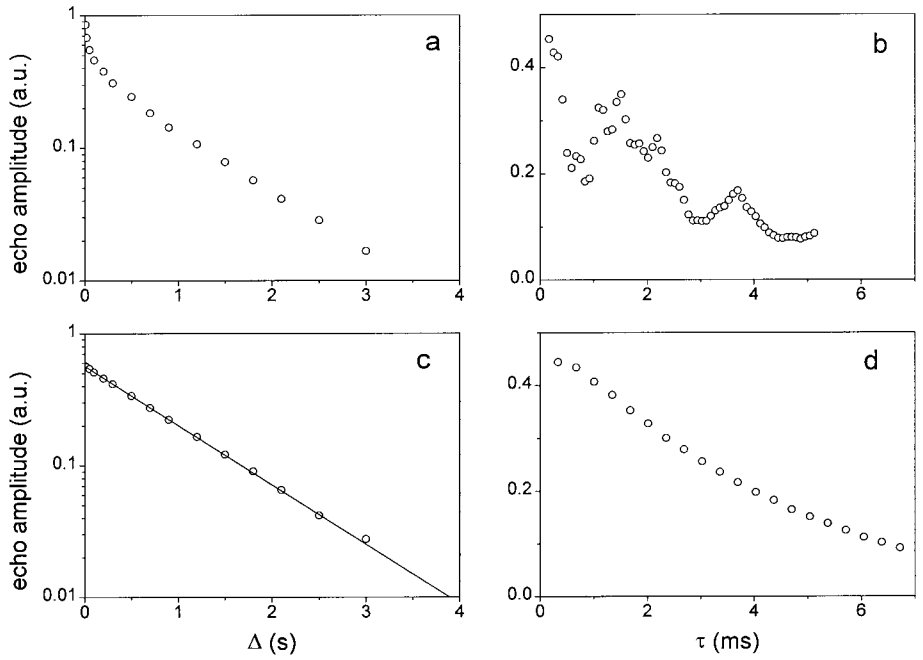

FIG. 5. Variation of the full ^{19}F signal intensity of CsPFO/D_2O in the nematic phase at 304 K, obtained from a PGSE experiment combined with homonuclear decoupling. The MREV-8 decoupling was performed with 2.6-μs-long 90° pulses and 84-μs-long cycles. The data were obtained by the pulse sequence in Fig. 1c (c, d), and with the same sequence but without the 180° rf pulses and with monopolar gradient pulses (a, b). Slice selection was performed by a soft Gaussian pulse of 20 kHz nominal bandwidth. In the first column (a, c) Δ is varied at constant $\tau = 1.68$ ms (corresponding to 20 MREV-8 cycles), while in the second column (b, d) τ is varied at constant $\Delta = 50$ ms. The line is a single-exponential fit.

problems are amplified in experiments with nuclei that have a wide chemical shift range. Note that ^1H experiments on high-field spectrometers are not immune from this problem either.

As usual, the improvements come at a price: bipolar gradient pulses are more demanding on the hardware, and because the gradient rise and fall times are doubled, they fill the encoding/decoding periods less effectively. The spectroscopist must choose judiciously. With older spectrometers one may not be able to generate bipolar gradient pulses (although sufficiently fast and robust switches for current reversal are relatively easy to build using MOS FETs). In that case cross-relaxation effects can still be suppressed by retaining the essential 180° pulses and by deleting the "negative" gradient pulses that follow them in Figs. 1b and 1c. The price is less effective gradient encoding.

EXPERIMENTAL

Cesium perfluorooctanoate (CsPFO) has been synthesized as described previously (*26*) and the sample has been produced by mixing CsPFO (40 wt%) with D_2O. The isotropic-nematic phase transition temperature was established to be 305 K.

The measurements were performed on a Bruker DMX 200 spectrometer, operating at 188 MHz for ^{19}F. We used a home-built gradient probe (*18, 27*). The length of the ^{19}F 90° pulse was 2.6 μs. The NOESY spectra were recorded with 50-μs increments in indirect dimension, and the TPPI algorithm was applied for recording phase-sensitive spectra. The MREV-8 sequence was sandwiched as $(45°)_{-y}$–(MREV-8)–$(45°)_{+y}$. The phases in the MREV-8 sequence were set to $+x$, $+y$, $-y$, $-x$, $-x$, $+y$, $-y$, $+x$ and were not cycled.

ACKNOWLEDGMENTS

This work has been supported by the Swedish Natural Science (NFR) and Engineering Science (TFR) Research Councils, and the Carl Trygger Foundation. S.V.D. thanks the Wenner–Gren Foundations for a scholarship.

REFERENCES

1. E. O. Stejskal and J. E. Tanner, Spin diffusion measurements: Spin echoes in the presence of a time-dependent field gradient, *J. Chem. Phys.* **42,** 288–292 (1965).
2. P. Stilbs, Fourier transform pulsed-gradient spin-echo studies of molecular diffusion, *Prog. NMR Spectrosc.* **19,** 1–45 (1987).
3. P. T. Callaghan, "Principles of Nuclear Magnetic Resonance Microscopy," Clarendon Press, Oxford (1991).
4. W. S. Price, Pulsed-field gradient nuclear magnetic resonance as a tool for studying translational diffusion: Part I. Basic theory, *Concepts Magn. Reson.* **9,** 299–336 (1997).
5. W. S. Price, Pulsed-field gradient nuclear magnetic resonance as a tool for studying translational diffusion: Part II. Experimental aspects, *Concepts Magn. Reson.* **10,** 197–237 (1998).
6. J. E. Tanner, Use of the stimulated echo in NMR diffusion studies, *J. Chem. Phys.* **52,** 2523–2526 (1970).

7. O. Söderman and P. Stilbs, NMR studies of complex surfactant systems, *Prog. NMR Spectrosc.* **26,** 445–482 (1994).
8. R. R. Ernst, G. Bodenhausen, and A. Wokaun, "Principles of Nuclear Magnetic Resonance in One and Two Dimensions," Clarendon Press, Oxford (1987).
9. C. S. Johnson, Effects of chemical exchange in diffusion-ordered 2D NMR spectra, *J. Magn. Reson. A* **102,** 214–218 (1993).
10. L. J. C. Peschier, J. A. Bouwstra, J. d. Bleyser, H. E. Junginger, and J. C. Leyte, Cross-relaxation effects in pulsed-field-gradient stimulated-echo measurements on water in a macromolecular matrix, *J. Magn. Reson. B* **110,** 150–157 (1996).
11. A. Chen and M. Shapiro, Nuclear Overhauser effect on diffusion measurements, *J. Am. Chem. Soc.* **121,** 5338–5339 (1999).
12. A. Chen, C. S. Johnson, M. Lin, and M. J. Shapiro, Chemical exchange in diffusion NMR experiment, *J. Am. Chem. Soc.* **120,** 9094–9095 (1998).
13. F. Grinberg, R. Kimmich, and S. Stapf, Investigation of molecular order and dynamics in liquid crystals confined in porous media using the dipolar-correlation effect on the stimulated echo, *Magn. Reson. Imaging* **14,** 883–885 (1996).
14. M. D. Pelta, H. Barjat, G. A. Morris, A. L. Davis, and S. J. Hammond, Pulse sequences for high-resolution diffusion-ordered spectroscopy (HR-DOSY), *Magn. Reson. Chem.* **36,** 706–714 (1998).
15. R. Kimmich, W. Unrath, G. Schnur, and E. Rommel, NMR measurement of small self-diffusion coefficients in the fringe field of superconducting magnets, *J. Magn. Reson.* **91,** 136–140 (1991).
16. I. Chang, G. Hinze, G. Diezemann, F. Fujara, and H. Sillescu, Self-diffusion coefficient in plastic crystals by multiple-pulse NMR in large static field gradients, *Phys. Rev. Lett.* **76,** 2523–2526 (1996).
17. S. V. Dvinskikh, R. Sitnikov, and I. Furó, ^{13}C PGSE NMR experiment with heteronuclear dipolar decoupling to measure diffusion in liquid crystals and solids, *J. Magn. Reson.* **142,** 102–110 (2000).
18. S. V. Dvinskikh and I. Furó, Combining PGSE NMR with homonuclear dipolar decoupling, *J. Magn. Reson.* **144,** 142–149 (2000).
19. R. F. Karlicek and I. J. Lowe, A modified pulsed gradient technique for measuring diffusion in the presence of large background gradients, *J. Magn. Reson.* **37,** 75–91 (1980).
20. D. Wu, A. Chen, and C. S. Johnson, An improved diffusion-ordered spectroscopy experiment incorporating bipolar-gradient pulses, *J. Magn. Reson. A* **115,** 260–264 (1995).
21. D. Canet, "Nuclear Magnetic Resonance. Concepts and Methods," Wiley, New York (1996).
22. D. Neuhaus and M. Williamson, "The Nuclear Overhauser Effect in Structural and Conformational Analysis," VCH, New York (1989).
23. S. J. Gibbs and C. S. Johnson, A PFG NMR experiment for accurate diffusion and flow studies in the presence of eddy currents, *J. Magn. Reson.* **93,** 395–402 (1991).
24. N. Boden, S. A. Corne, and K. W. Jolley, Lyotropic mesomorphism of the cesium pentadecafluorooctanoate/water system: High-resolution phase diagram, *J. Phys. Chem.* **91,** 4092–4105 (1987).
25. R. Raulet, I. Furó, J. Brondeau, B. Diter, and D. Canet, Water–surfactant contact studied by ^{19}F–^{1}H heteronuclear Overhauser effect spectroscopy, *J. Magn. Reson.* **133,** 324–329 (1998).
26. H. Jóhannesson, I. Furó, and B. Halle, Orientational order and micelle size in the nematic phase of the cesium pentadecafluorooctanoate–water system from the anisotropic self-diffusion of water, *Phys. Rev. E* **53,** 4904–4917 (1996).
27. I. Furó and H. Jóhannesson, Accurate anisotropic water diffusion measurements in liquid crystals, *J. Magn. Reson. A* **119,** 15–21 (1996).
28. M. Mehring, "Principles of High Resolution NMR in Solids," Springer-Verlag, Berlin (1983).